**Belgacem AIS[1,2],Tayeb ALLAOUI[2],Abdelkader CHAKER[1],Abderrahmane HEBIB[1],Belkacem BELABBAS[2], Lalia MERABET[1]**

Department of Electrical Engineering, Faculty of Electrical Engineering,SCAMRE Laboratory,ENP,Oran,31000,Algeria (1),
Department of Electrical Engineering, Faculty of Applied Science,L2GEGI Laboratory, University of TIARET,Tiaret,14000, Algeria (2)

doi:10.15199/48.2021.04.12

# Contribution to the optimization and control of a Photovoltaic system connected to the Grid based a five levels inverter

***Abstract**. This paper is aimed to optimizing and improving the performance of a Photovoltaic system connected to the Grid based a five levels inverter using conventional and advanced methods. The MPPT methods considered in this study include Sliding Mode Control (SMC) and Perturb and Observe (PO). We used a five level inverter controlled by passive methods to connect the PV system to the grid. The DC link voltages are controlled by using a closed loop called clamping bridge and an adaptive fuzzy logic PI controller (AFLC-PI). A PV model and power converters are modeled in Matlab SimpowerSystems toolbox and the MPPT and control algorithms are tested under different operating conditions to analyze the performance and limitations of each algorithm.*

***Streszczenie**. Artakuł analizuje możliwościoi poprawy właściwości i optymalizacji systemu fotowoltaicznego podłączonego do sieci I bazującego na przekształtniku piątego rzędu. Wykorzystano metodę MPPT (Maximum Power Point Tracking), sterowanie ślizgowe SMC. System is modelowany w Matlabie Simpopwer System Toolbox . (**Optymalizacja systemu fotowoltaicznego podłączonego do sieci bazującego na przekształtniku piatego rzędu**)*

**Keywords:** PV system, Sliding mode control, Adaptive PI Fuzzy Logic, Passive E-L Model, Five levels Inverter.
**Słowa kluczowe**: system fotowoltaiczny, przekształtnik, MMMT – nmaxum Power Point Tracking

## 1. Introduction

The rapid increase in the demand for electricity and the recent change in the environmental conditions such as global warming led to a need for a new source of energy that is cheaper and sustainable with less carbon emissions [1, 6].

For low and medium voltages, the use of conventional two-level converters with high switching frequencies appears to be limited due to significant losses caused by switching switches, the multilevel inverters have been put into address this problem and have several advantages: improvement of energy quality, reduction of harmonic distortion, reduction of electromagnetic compatibility, increase in power [8].

Multilevel converters have attracted increasing attention in medium-voltage and high-power applications such as renewable energy sources, especially in developing high-power generators. Three major topologies are used in high-power applications [buck to buck]: the neutral-point (NP) clamped (NPC), flying capacitor, and cascaded H-bridge converters. Among them, the NPC topology is the most widely used [9], because of its simple construction and merely single DC source requirement.

In the literature, there are several control and control regulators for DC/DC and DC/AC converters to obtain an output inverter voltage approaching a perfect sine wave form using the SPWM modulation method based on development of classical and modern control theories applied to the inverter such as: (passive E-L model, Fuzzy Logic (FLC), and adaptive dual integrated mod control) [8].

The passive E-L model of passivity has a better robustness and dynamic with the traditional PI in this context, new command will be added to this document which will be studied, analyzed and compared and then evaluate then the advantages and disadvantages of these presented commands [11].

The main contributions of the paper are as follow:

- A simple MPPT based on sliding mode based to track the maximum power from PV.
- Use the five levels NPC inverter.
- Control the DC voltage of DC-link by an adaptive PI fuzzy logic controller.
- Control a five level inverter controlled by a Passive E-L methods.

The paper is organised as follows: Section 2 describes the proposed PV system connected to the AC bus through a three-phase by five-level DC-AC inverter. Section 3 of the paper presents the PV model. A brief description of the PV system and its maximum power point tracking (MPPT) control using P&O and sliding mode techniques are presented in Section 4. The modelling of the NPC five level inverters is developed and explained in Section 5. The design of Passive E-L Model Controller and an adaptive fuzzy logic PI controller of the Five-Level Inverter are presented in section 6 and 7 respectively. The simulation results are presented in Section 8 and finally discussions and conclusions are given in Section 9.

## 2. Description Of PV System Based A Five Levels Inverter

The configuration of a grid connected PV system is illustrated in Fig.1, depicts the block diagram of the complete control circuits. In this work, the sinusoidal pulse width modulation (SPWM) is used to control the inverter because this power system needs a fixed frequency for switching.

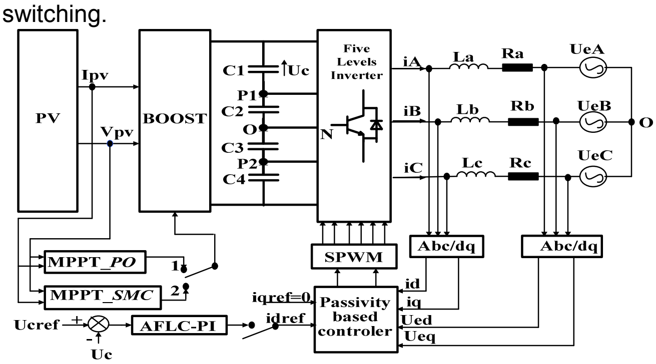


Fig 1. PV system connected to the grid by a five levels invetrer.

## 3. Modeling Of The PV Array

Fig 2. Shows the equivalent circuit of the ideal photovoltaic cell.

Applying Kirchhoff's current law, the terminal current of the cell is [2, 10]

(1) $$I = Ipv - I_d - I_R$$

(2) $$I_R = \frac{V + R_S I}{R_P}$$

The junction current is given by:

(3) $$I_R = \frac{V + R_S I}{R_P}$$

The formula the current and voltage in the circuit is:

(4) $$I = I_{pv} - I_0 \left[ \exp\left( \frac{V + R_S I}{V_t . a} \right) - 1 \right] - \frac{V + R_S I}{R_P}$$

(5) $$Vt = \frac{N_S . K . T}{q}$$

The light generated current of the PV cell is given by:

(6) $$I_{pv} = \left( I_{pv,n} + K_I . \Delta_T \right) + \frac{G}{G_n}$$

The diode saturation current and its dependence on the temperature may be expressed by:

(7) $$I_0 = \frac{I_{SC,n} + K_I . \Delta_T}{\frac{I_{OC,n} + K_V . \Delta_T}{a . V_t} - 1}$$

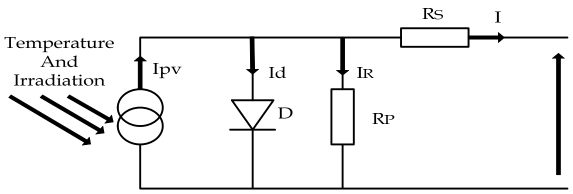

Fig 2. Equivalent Circuit of Solar PV Cell

## 4. Mode DC-DC Converter and Maximum Power Point Tracking (MPPT)

Fig. 3 shows the basic circuit configuration of a DC-DC boost converter with an MPPT controller. A capacitor is generally connected between PV panel and the boost circuit to reduce high frequency harmonics.

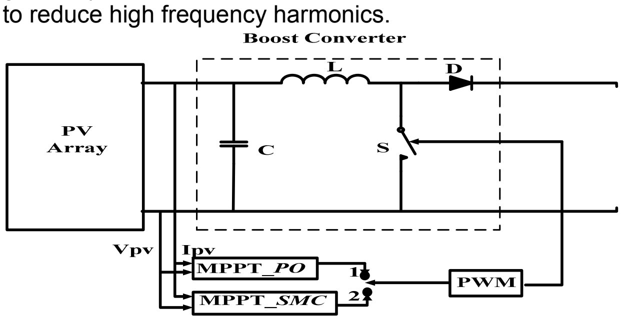

Fig 3. Boost circuit and MPPT controller.

### 4.1 MPPT based on P&O

Table 1 summarizes the operation of the P&O algorithm

Table 1. The operation of the P&O algorithm.

| Case | dPpv | dVpv | Action | duty cycle |
|---|---|---|---|---|
| 1 | P(k) > P(k-1) | V(k) > V(k-1) | V++ | D-- |
| 2 | P(k) > P(k-1) | V(k) <V (k-1) | V-- | D++ |
| 3 | P(k) < P(k-1) | V(k) > V(k-1) | V-- | D++ |
| 4 | P(k) < P(k-1) | V(k) <V (k-1) | V++ | D-- |

### 4.2 MPPT based on SMC

The first step of SMC design is to select a sliding surface that models the desired closed-loop performance in state variable space. Then the control should be designed such that the system state trajectories are forced towards the sliding surface and stay on it. The system state trajectory during the period of time before reaching the sliding surface is called the reaching phase. Once the system trajectory reaches the sliding surface, it stays on it and slides along it to the origin. The system trajectory sliding along the sliding surface to the origin is the sliding mode. The structure of a sliding mode controller is defined by [6]:

(8) $$U = U_{eq} + U_n$$

$U_{eq}$ is called equivalent control. $U_n$ is called normal control.

The structure of a sliding mode controller is defined by [12]:

(9) $$U = \alpha(k+1) \text{ and } U_{eq} = \alpha(k)$$

With: $\alpha(k+1)$ and $\alpha(k)$ is the duty cycle in the instants $k$ and $k+1$ respectively.

The switching function (S) defined as:

(10) $$S = \frac{\partial P_{pv}}{\partial V_{pv}}$$

(11) $$P_{pv} = V_{pv} . I_{pv}$$

Substituting equation (11) in equation (10) gives:

(12) $$S = \frac{\partial (V_{pv} * I_{pv})}{\partial V_{pv}} = V_{pv} \left( \frac{\partial P_{pv}}{\partial V_{pv}} + \frac{I_{pv}}{V_{pv}} \right)$$

The switching function in the instant $k$ and $k+1$ respectively becomes:

(13) $$S = V_{pv} \left( \frac{I_{pv}(k) - I_{pv}(k-1)}{V_{pv}(k) - V_{pv}(k-1)} + \frac{I_{pv}(k)}{V_{pv}} \right)$$

The duty cycle of boost is:

(14) $$\alpha = 1 - \frac{V_{in}}{V_{out}}$$

The equivalent control of the MPPT_SMC is the expression for the duty cycle is obtained as follows:

(15) $$U_{eq} = \alpha$$

The normal control $U_n$ it is defined as:

(16) $$U_n = k * sign(S)$$

$k$ is a positive constant, representing the maximum controller output required to overcome parameter uncertainties and disturbances. The basic SMC scheme is shown in Fig. 4.

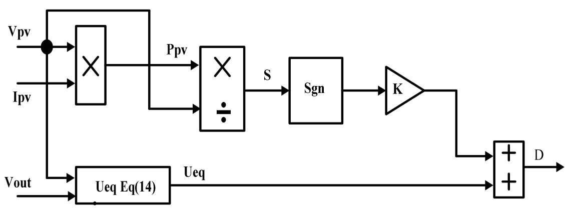

Fig 4. Building bloc and structure of a SMC

## 5. Modeling Of The PV System

The basic architecture of topology of the diode-clamped five-level inverter is shown in Fig. 5 [11].

(17)
$$\begin{cases} L_f \dfrac{di_k}{dt} + Ri_k - \left[(Sk_1 + Sk_2)U_{C1} - (Sk_7 + Sk_8)U_{C4}\right] + U_{ON} = -U_{ek} \\ C\dfrac{dU_{C1}}{dt} + S_{A1}i_A + S_{A2}i_A + S_{B1}i_B + S_{B2}i_B + S_{C1}i_C + S_{C2}i_C = I_{dc} \\ C\dfrac{dU_{C4}}{dt} - S_{A1}i_A - S_{A2}i_A - S_{B1}i_B - S_{B2}i_B - S_{C1}i_C - S_{C2}i_C = I_{dc} \end{cases}$$

There fore

(18)
$$U_{ON} = \frac{1}{5}\begin{bmatrix} (S_{A1} + S_{A2} + S_{B1} + S_{B2} + S_{C1} + S_{C2} +)U_{C1} \\ -(S_{A7} + S_{A8} + S_{B7} + S_{B8} + S_{C7} + S_{C8} +)U_{C4} \end{bmatrix}$$

where UC1 and UC4 are the voltages of the capacitors C1 and C4 in the DC side, respectively, and iA, iB, and iC are the three-phase current of the inverter. After the coordinate transformation.

(19)
$$\begin{cases} L_f \dfrac{di_d}{dt} + wL_f i_q + Ri_d - \left[(S_{d1} + S_{d2})U_{C1} - (S_{d7} + S_{d8})U_{C4}\right] = -U_{ed} \\ L_f \dfrac{di_q}{dt} + wL_f i_d + Ri_q - \left[(S_{q1} + S_{q2})U_{C1} - (S_{q7} + S_{q8})U_{C4}\right] = -U_{eq} \\ \dfrac{3}{5}C\dfrac{dU_{C1}}{dt} + (S_{d1} + S_{d2})i_d - (S_{q1} + S_{q2})i_q = \dfrac{3}{5}I_{dc} \\ \dfrac{3}{5}C\dfrac{dU_{C4}}{dt} - (S_{d7} + S_{d8})i_d - (S_{d7} + S_{d8})i_q = \dfrac{3}{5}I_{dc} \end{cases}$$

Table 2. Terminal Voltage Switching state

| Terminal Voltage Switching state | | | | | |
|---|---|---|---|---|---|
| | +Udc/2 | +Udc/4 | 0 | -Udc/4 | -Udc/2 |
| TA1 | ON | OFF | OFF | OFF | OFF |
| TA2 | ON | ON | OFF | OFF | OFF |
| TA3 | ON | ON | ON | OFF | OFF |
| TA4 | ON | ON | ON | ON | OFF |
| TA5 | OFF | ON | ON | ON | ON |
| TA6 | OFF | OFF | ON | ON | ON |
| TA7 | OFF | OFF | OFF | ON | ON |
| TA8 | OFF | OFF | OFF | OFF | ON |

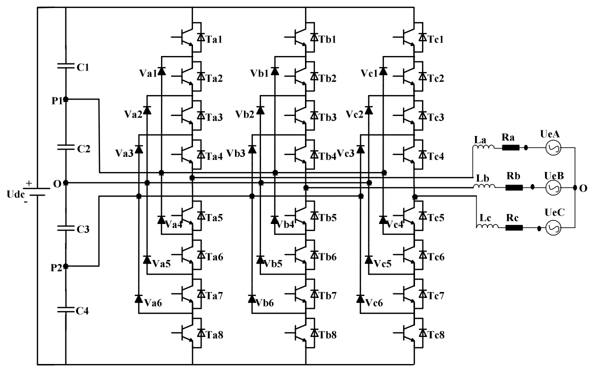

Fig.5. The topology of the diode-clamped five-level inverter

## 6. Design Of E-L Passive Model Controller Of The Five Level Inverter

Selecting the system's state variables [11]:

(20) $X = \begin{bmatrix} x_1 & x_2 & x_3 & x_4 \end{bmatrix} = \begin{bmatrix} i_d & i_q & U_{C1} & U_{C4} \end{bmatrix}$

Defining the energy storage function of the system:

(21) $H(x) = \begin{bmatrix} x_1^2 & x_2^2 & x_3^2 & x_4^2 \end{bmatrix} / 2$

Equation (19) is written in the form of the E-L equation under passivity-based controls (see Figure 5)

(22) $M\dot{x} + jx + Rx = U$

According to the autor [11] and after combinations of the preceding equations with the E-L équation, it can be deduced:

(23)
$$\begin{cases} U_d = -wL_f i_q + (R + R_{a1})i_{dref} - R_{a1}i_d + U_{ed} \\ U_q = wL_f i_d - R_{a2}i_q + U_{ed} \end{cases}$$

## 7. An Adaptive Fuzzy Logic PI Controller

The gains of the PI controller are adjusted online using the FLC [3]

The membership functions for the inputs and outputs variables are of triangulaire shape and are represented in Fig. 7 and 8.

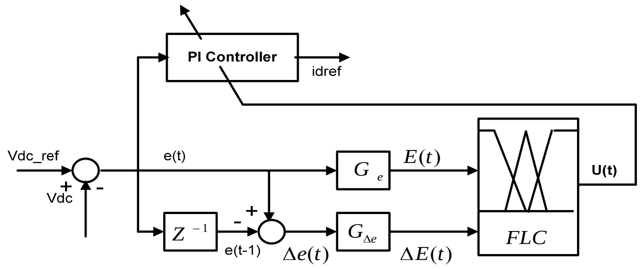

Fig.6. Structure of the adaptive fuzzy logic PI controller

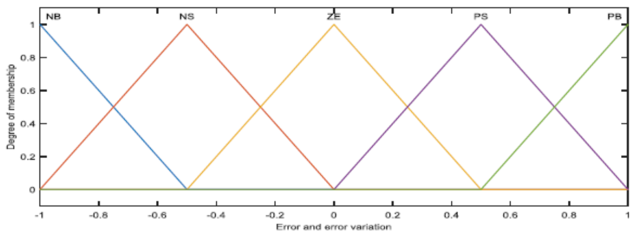

Fig.7. Membership functions of e and of Δ e.

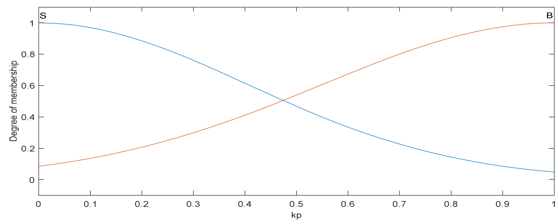

Fig.8. Membership functions of kp and of ki.

This strategy is performed by the rule base matrix given by Table 3.

Table 3. The rule base matrix

| e | Δe | | kp | Ki |
|---|---|---|---|---|
| NB | NB | | S | S |
| NB | NS | | S | S |
| NB | ZE | | S | S |
| NB | PS | | S | S |
| NB | PB | | S | S |
| NS | NB | | B | B |
| NS | NS | | B | B |
| NS | ZE | | B | B |
| NS | PS | | B | B |
| NS | PB | | B | B |
| ZE | NB | | S | S |
| ZE | NS | | S | S |
| ZE | ZE | | S | S |
| ZE | PS | | S | S |
| ZE | PB | | S | S |
| PS | NB | | B | B |
| PS | NS | | B | B |
| PS | ZE | | B | B |
| PS | PS | | B | B |
| PS | PB | | B | B |
| PB | NB | | S | S |
| PB | NS | | S | S |
| PB | ZE | | S | S |
| PB | PS | | S | S |
| PB | PB | | S | S |

## 8. Simulation Results And Discussion

The PV conversion system, the grid side control strategies and MPPT control schemes studied are simulated in Matlab/Simulink and SimpowerSystem toolbox with the parameters given in the Appendix. This simulation study will be based on two test: (i) MPPT_PO with PI adaptive fuzzy logic control base on passive E-L model, (ii) MPPT_sliding mode control with PI adaptive fuzzy logic control based E-L model.

The line voltage waveform of the inverter is presented in Fig 9, consists of + 700V, +525V, +350V, 175V, 0V, -175V, -350V, -525V, -700V, whitch is respectively close to the five levels of the inverter output in theory, whitch are +Vdc, + 3/4Vdc, + 1/2Vdc, + 1/4Vdc, 0, -1/4Vdc, -1/2Vdc, -3/4Vdc, and -Vdc

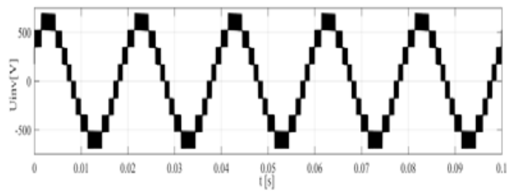

Fig 9. line voltage waveform inverter.

According to the Fig.10, it will be confirmed that the I_load current is the sum of I_source current and I_inverter wave current regardless of the load variation. Between:

Table 4. current system as a function of load variation.

| Load variation and Time variation | Current System |
|---|---|
| t=0 and t=0.4s<br>load=10kw | I_load=65A<br>I_grid=55A<br>I_inv=10.6A |
| t=0.4s and t=0.8s<br>load=12kw | I_load=78A<br>I_grid=68A<br>I_inv=10.6A |
| t=0.8s and t=1s<br>load=14kw | I_load=91A<br>I_grid=68A<br>I_inv=10.6A |

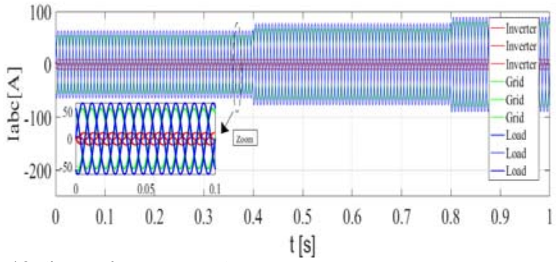

Fig 10. three phase current

The Ppv power from the pannel photovoltaic is shown in Fig.11, under two control strategies. As can be seen from the figure, P tends to be stable at about 0.002s, and the stability value is close to 4800 W under the two control strategies.

However, fluctuation in the amplitude of Ppv power in control strategie (MPPT_PO with PI adaptive Fuzzy logic side grid) is significant and with chattering between (4540w to 4815w), ΔP=275w. However in the control strategie (MPPT_smc with adaptive Fuzzy logic control) is very good with chattering between (4811 w – 4813 w), ΔP =2 w.

It can be concluded that the static stability of these last control strategie based on (MPPT_smc with PI adaptive fuzzy logic mode control) is very good. The Vdc voltage from the inverter is shown in Fig 12, under two control strategies. As can be seen from the figure, Vdc is stabil value is (700/4) V for the two control strategies. However, the amplitude fluctuations of the voltage for the control strategie (MPPT_PO with PI AFLC) is larger than those an other control strategie (MPPT_SMC with PI AFLC). It can be concluded that the static stability of the control strategie (MPPT_SMC with PI AFLC) is good.

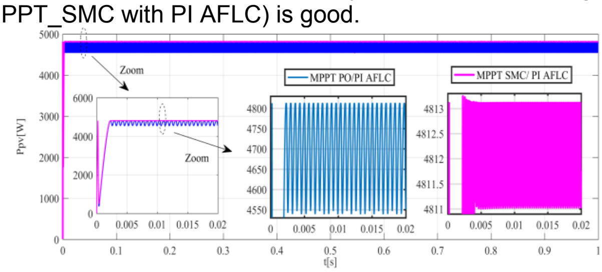

Fig 11. Potovoltaique power.

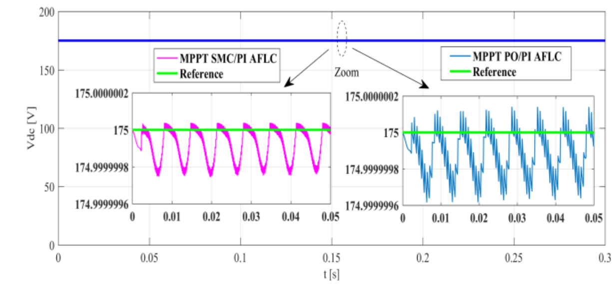

Figure 12. voltage Vdc inverter.

The Vout voltage from the boost is shown in Fig.13, under two control strategies. As can be seen from the figure, Vout is stable value is 700 V for the two control strategies. However, the amplitude fluctuations of the voltage for the control strategie (MPPT_PO with PI AFLC) is larger than those an other control strategies (MPPT_SMC with PI AFLC). It can be concluded that the static stability of the control strategie (MPPT_SMC with PI AFLC) is good.

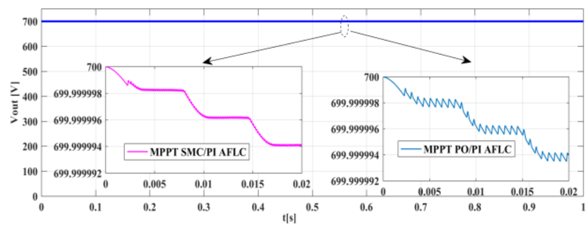

Fig 13. Output voltage Boost.

According to the Fig.14, it will be confirmed that the Pload power is the sum of Pgrid power and Pinverter power regardless of the load variation. Between:

Table 5. Power system as a function of time variation.

| time variation | Power System |
|---|---|
| t=0 and t=0.4s | P_load=10kw<br>P_grid=8455w<br>P_inv=1545w |
| t=0.4s and t=0.8s | P_load=12kw<br>P_grid=10455w<br>P_inv=1545w |
| t=0.8s and t=1s | P_load=14kw<br>P_grid=12455w<br>P_inv=1545w |

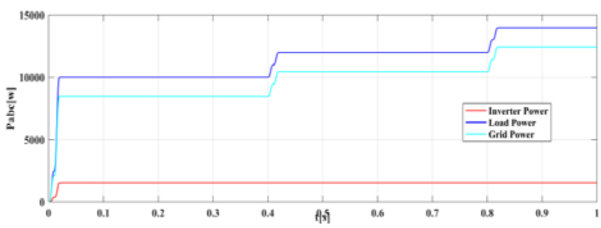

Fig 14. Power system.

## 9. Conclusions

This paper is related to optimize and control of a Photovoltaic system connected to the Grid based a five levels inverter for improve the electrical performance using conventional and advanced methods.

The P&O algorithm is a classic and simple algorithm. In general, this algorithm strongly depends on the initial conditions and it presents oscillations of the tension, but the SMC algorithm is a robust and efficient algorithm. Indeed, these algorithm works at the optimal point without oscillations. In addition, it is characterized by good transient behaviour.

The simulation results show that improved performance has been achieved by these algorithms as compared to P&O. P&O method can cause large ondulation caused by discontinuous control law and a of the parametrs system are actually known. SMC, PI_AFLC methods provides better performance and robustness even under large load changes.

The passivity-based control strategy using adaptive PI fuzzy logic control (PI_AFLC) has better static and dynamic stability and makes the system achieve a higher power factor.

In terms of economy, the harmonic loss very small under passivity-based control using adaptive PI fuzzy logic (PI_AFLC) and sliding mode control (MPPT_SMC).

***ACKNOWLEDGEMENTS***

*This work was supported by SCAMRE laboratory at Polytechnic national school (Oran, Algeria) in collaboration with L2GEGI laboratory at the University Ibn-Khaldun (Tiaret, Algeria).*

*Authors:*
*Belgacem AIS[1], Tayeb ALLAOUI[2] ,Abdelkader CHAKER[1] ,Abderrahmane HEBIB[1] ,Belkacem BELABBAS[2] , Lalia MERABET[1]*
*Department of Electrical Engineering, SCAMRE Laboratory,ENP,Oran,31000,Algeria (1),*
*Department of Electrical Engineering, L2GEGI Laboratory, University of TIARET,Tiaret,14000, Algeria (2)*

REFERENCES

[1] Prof.R.Arulmurugan, Dr.N.Suthanthira Vanitha, (2013). Fuzzy Logic Controller with Maximum Power Point Tracking using Creative Design of DC to DC Buck Converter for Photovoltaic Power System, And electricals Engineering, Elsevier.

[2] M. G. Villalva, J. R. Gazoli, E. Ruppert F. (2009). Modeling and Circuit-Based Simulation Of Photovoltaic ARRAYS , vol. 14, no. 1,Brazilian journal of power electronics, pp. 35-45.

[3] Abdeldjabbar Mohamed Kouadria, T. Allaoui, M. Denaï and G. Pissanidis. « Power Quality Enhancement in Off-Grid Hybrid Renewable Energy Systems Using Type-2 Active Filter » 2016, Springer International Publishing. The title of the book: Intelligent Systems and Applications.

[4] M. Arsalan, R. Iftikhar, I. Ahmad, A. Hasan, K. Sabahat, et A. Javeria, (2018). MPPT for photovoltaic system using nonlinear backstepping controller with integral action, vol.170, p.192–200, Sol. Energy.

[5] Q. Mei, M. Shan, L. Liu, et J. M. Guerrero, (2011). A Novel Improved Variable Step-Size Incremental-Resistance MPPT Method for PV Systems, vol. 58, no.6, Ind. Electron. IEEE Trans. On, p. 2427–2434.

[6] B. Belabbas, T. Allaoui, M. Tadjine, et M. Denai, (2017). Power Quality Enhancement in Hybrid Photovoltaic-Battery System based on three–Level Inverter associated with DC bus Voltage Control , J. Power Technol., vol. 97, no 4, p. 272–282.

[7] Karuna Mudliyar, Suryanarayana K, H.V.Gururaj Rao, L.V Prabhu, Krishnaprasad, (2013). Analysis of High Frequency Multi- Phase Multi-Stage Boost Converter, Vol.2, no.1 International Journal of Advanced Electrical and Electronics Engineering, (IJAEEE).

[8] Sohaib Tahir, JieWang , Mazhar Hussain Baloch, Ghulam Sarwar Kaloi, (2018). Digital Control Techniques Based on Voltage Source Inverters in Renewable Energy Applications: A Review www.mdpi.com/journal/electronics

[9] Chabakata MAHAMAT, Mickaël PETIT, François COSTA, (2017). Balanced Active and Reactive Control Applied to a Grid Connected Five Level Inverter», **Vol.8**, no.10, (IJACSA) International Journal of Advanced Computer Science and Applications.

[10] B. Belabbas, T. Allaoui, M. Tadjine, et M. Denai, (2017). Power management and control strategies for off-grid hybrid power systems with renewable energies and storage , Energy Syst., p. 1–30.

[11] Tao Li; Qiming Cheng ; Weisha Sun ; Lu Chen «Grid-Connected Control Strategy of Five- level Inverter Based on Passive E-L Model » , Energies, 2017